

Precambrian Microcontinents of the Ural–Mongolian Belt: New Paleomagnetic and Geochronological Data

N. M. Levashova^a, A. S. Gibsher^b, and J. G. Meert^c

^a *Geological Institute, Russian Academy of Sciences, Pyzhevskii per. 7, Moscow, 119017 Russia*

e-mail: namile2007@rambler.ru

^b *Institute of Geology and Mineralogy, Siberian Branch, Russian Academy of Sciences,
pr. Akad. Koptyuga 3, Novosibirsk, 630090 Russia*

^c *Department of Geological Sciences, University of Florida, 274 Williamson Hall, Gainesville, FL, 32611 USA*

Received May 14, 2009

Abstract—The knowledge on the early stages of evolution of the Ural–Mongolian Belt (UMB) (Late Neoproterozoic–Cambrian) is a key for understanding of its evolution in the Paleozoic. Unfortunately, this stage remains poorly studied. The tectonic reconstructions of the UMB for this time primarily depend on the views on the kinematics and tectonic evolution of numerous sialic massifs with Precambrian basement in the structure of the Tien Shan, Kazakhstan, Altai, and Mongolia. At present, the concept of the origin of these massifs is largely based on the lithostratigraphic similarity of the Neoproterozoic and Lower Paleozoic sections of the Tarim, South China, and Siberian platforms with coeval sections of Precambrian massifs within the UMB. New paleomagnetic and geochronological data can serve as additional sources of information on the origin and paleotectonic position of the microcontinents. In this paper, we present new isotopic datings and a new paleomagnetic determination for the Neoproterozoic volcanic rocks of the Zabhan Formation from the Baydrag microcontinent in central Mongolia. It is established that 805–770 Ma ago (U–Pb LA-MC-ICP-MS age of zircon) the Baydrag microcontinent was situated at a latitude of $47 \pm 14^\circ$ in the Northern or Southern hemisphere. These data provide new insights into the possible origin of the Precambrian microcontinents in the UMB. Analysis of paleomagnetic data and comparison of the age of the basement beneath various plates allow us to state rather confidently that ~800 Ma ago the microcontinents of the UMB belonged to one of the North Rodinian plates: Indian, Tarim, or South China; their Australian origin is less probable.

DOI: 10.1134/S0016852111010043

INTRODUCTION

The Ural–Mongolian Belt (UMB) situated between the East European Platform and Siberian, Tarim, and North China cratons (Fig. 1a) is one of the most extended and complexly built mobile zones of the Earth. The central part of the UMB is composed of the Neoproterozoic, Salairian, Caledonian, and Variscan tectonic units of Kazakhstan, the Altai–Sayan region, and most of Mongolia (Fig. 1b). The Early Paleozoic structure of the central part of the belt is often called mosaic because fragments of the fold zones are variously oriented and often strike in perpendicular directions. Abutted junctions along large wrench faults are widespread. Common is tectonic juxtaposition of Precambrian sialic massifs overlapped by cherty–terrigenous–carbonate covers with Paleozoic island-arc volcanic series, flysch sequences, and accretionary complexes.

The published models of the tectonic evolution of the UMB are diverse. One group of models is based on the idea of the existence of the Late Neoproterozoic–Early Paleozoic Paleoasian ocean with numerous

microcontinents separated by island arcs and backarc basins. The main role in the formation of the foldbelt is assigned to opening and closure of the oceanic and backarc basins and, as a consequence, to multistage collisions of microcontinents and island arcs. According to [8, 29], most of these blocks were attached to the Siberian Platform in the Ordovician and Silurian with the formation of the composite Siberian–Kazakh continent. In other publications, e.g., [28, 41], these blocks collided with one another, forming the Kazakh continent, which then traveled independently of the other plates.

Another group of models suggests that extended volcanic belts existed between the European and Siberian cratons [20, 75, 79, 91, 92]. These models are based on the assumption that a giant island-arc system (Kipchak arc) existed in the late Neoproterozoic–Early Paleozoic and the movement of this arc was coordinated with Baltica and Siberia. Since the end of the Ordovician, the structure of this system has been complicated due to the attachment of extensive accretionary complexes and longitudinal juxtaposition of

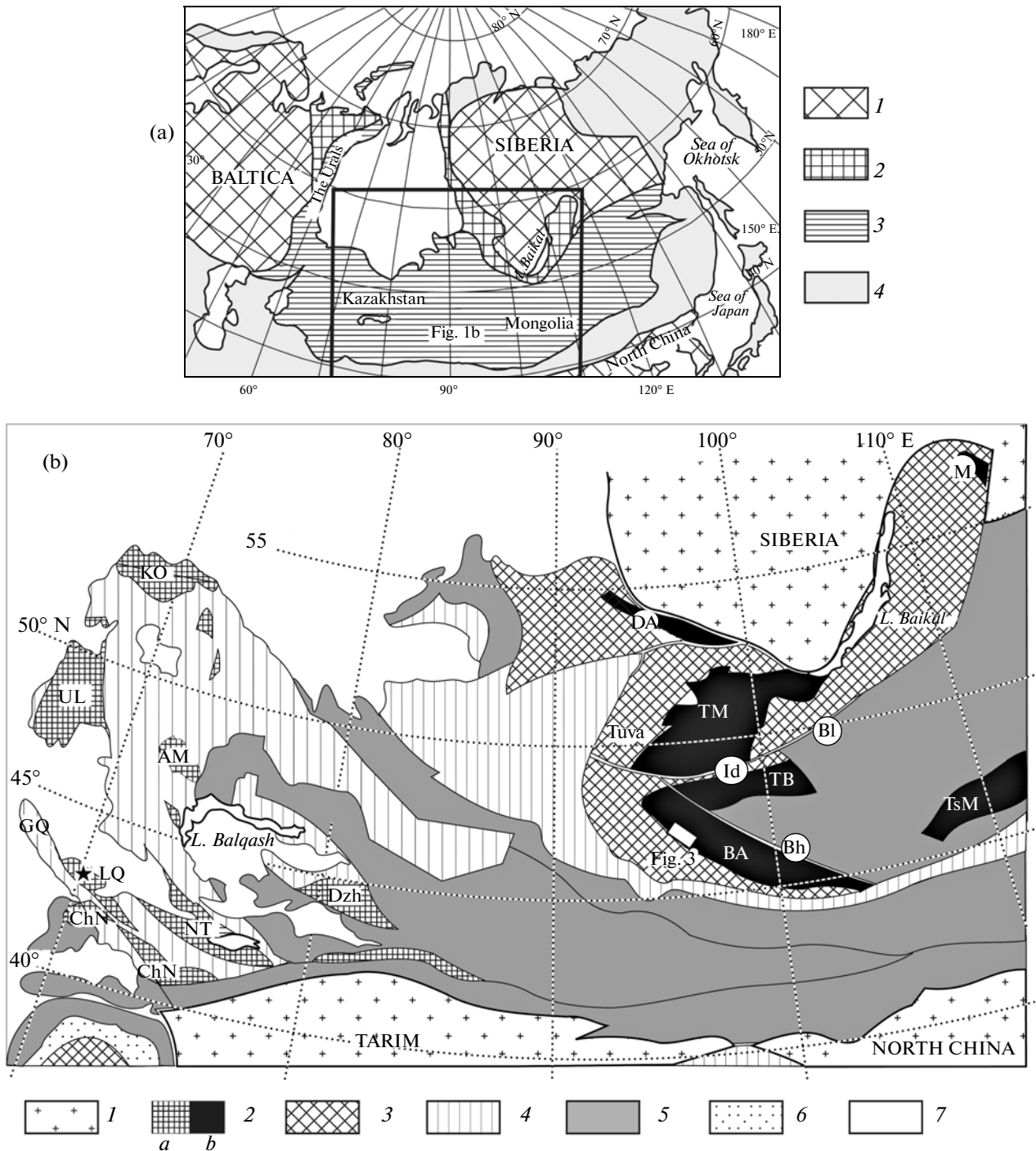


Fig. 1: (a) Tectonic scheme of Eurasia and (b) simplified scheme of the Ural–Mongolian Belt, after [20]. Panel (a): (1) craton, (2) Late Precambrian mobile belt, (3) Ural–Mongolian Fold Belt; (4) other tectonic zones. Panel (b): (1) main cratons; (2) microcontinents: (a) in the west of Kazakhstan, (b) to the south of Siberia; (3) Early Paleozoic foldbelt; (4) Middle Paleozoic foldbelt; (5) Late Paleozoic foldbelt; (6) Mesozoic and Cenozoic cover. Microcontinents (hatched in Kazakhstan and black to the south of Siberia and in Mongolia) (letters in figure): AM, Aqtau–Moynty; BA, Baydrag; TsM, Central Mongolian; ChN, Chatkal–Naryn; DA, Derbina–Arzybey; GQ, Greater Qaratau; Dzh, Zhungar; KO, Kokshetau; LQ, Lesser Qaratau; M, Muya; NT, North Tien Shan; TB, Tarbogatai; TM, Tuva–Mongolian; UL, Ulutau; letters in circles: Id, Ider Belt; Bh, Bayanhongor ophiolite belt; Bl, Bolnay Fault. The area of sampling for paleomagnetic determinations in the Lesser Qaratau [48] is marked by a star.

particular segments of the arc. A structural unit, which can be identified as the Kazakh continent, was formed in the Carboniferous. As is supposed in [91, 92], two parallel island arcs existed, whereas according to [20, 79], the Early Paleozoic island arcs had a complex configuration and their echeloning is not as important as inferred in [75].

None of the existing models explains the entire body of available information. Biostratigraphic data also do not give preference to any model because the spatial localization of different faunal taxons corresponds to the combination of various models [4].

The knowledge on the early stages of evolution of the UMB (Late Neoproterozoic–Cambrian) is a key for understanding of its evolution in the Paleozoic. Unfortunately, this stage remains poorly studied. The lithostratigraphic similarity of the Neoproterozoic–Cambrian sections of different microcontinents in the UMB was established long ago [1, 12], but different authors have arrived at quite different conclusions on the basis of these data. Some of them have suggested that the microcontinents initially belonging to the eastern margin of Gondwana were detached from it in the Neoproterozoic (1000–650 Ma ago) and traveled across the Paleasian ocean to collide with Siberia or the hypothetical continent of Kazakhstan [8, 9, 41]. On the basis of the same data, Berzin and Dobretsov [28] suggested that all of the microcontinents belonging to Siberia were separated from the latter 800–600 Ma ago and again attached to it at the end of the Neoproterozoic. It has also been suggested that some microcontinents could have broken off from Baltica and others from Siberia [75].

To ascertain the origin of the Precambrian microcontinents, paleomagnetic evidence is of particular importance. Unfortunately, such evidence remains extremely limited. New geochronological and paleomagnetic data on the Neoproterozoic complexes of the Lesser Qaratau microcontinent in Central Kazakhstan are presented in [48]. The acid tuffs of the Qurgan Formation have a U–Pb zircon age of 805–770 Ma. The Lesser Qaratau microcontinent was located at that time at a latitude of $34.2 \pm 5.3^\circ$ N or S.

The carbonate rocks of the Ediacaran Tsagaan-Olom Formation from the Baydrag microcontinent in Central Mongolia (Fig. 1b) have been studied twice [31, 46]. It is noteworthy that the authors of the first publication [31] managed to separate only the secondary components of magnetization, whereas the authors of the latter publication [46], having studied the same rocks, separated a certain component of magnetization, which was classified as the primary one. Unfortunately, this result has not been confirmed in any field tests. Because no other data are available, we have to mention that according to [46], the Baydrag microcontinent was located in the Late Ediacarian–Early Cambrian at equatorial latitudes.

In our paper, we present a new paleomagnetic determination and isotopic geochronological data on the Neoproterozoic volcanic rocks of the Zabhan Formation from the Baydrag microcontinent in Central Mongolia and use these data to specify the possible origin of the Precambrian microcontinents in the UMB.

PRECAMBRIAN SIALIC MASSIFS OF THE URAL–MONGOLIAN BELT

In the UMB, Precambrian sialic massifs cluster largely in the west of Central Kazakhstan, in the North Tien Shan, and south of the Siberian Platform (Fig. 1b). The western group comprises the Kokshetau, Ulutau, Lesser Qaratau, Zhungar, Greater Qaratau, Chatkal–Naryn, and Aqtau–Moynty sialic massifs along with a number of smaller blocks. The Baydrag and Tarbogatay blocks, the Gargan Block of the Tuva–Mongolian Massif, as well as the Derbina–Arzybey and Central Mongolian microcontinents, are localized to the south of Siberia.

The basements of most massifs are composed of Proterozoic sequences similar in structure, composition, and age. The Middle and Upper Neoproterozoic quartzites, slates, and carbonate rocks are typical (the Kokshetau Group and its analogues) [7]. It should be noted, however, that the proved age of the basement varies from Archean and Paleoproterozoic to Early Neoproterozoic. The Archean and Paleoproterozoic age of the basement is proved only for the Baydrag, Ulutau, and North Tien Shan microcontinents [47]. The Tuva–Mongolian composite massif comprises the Paleoproterozoic Gargan Block (U–Pb zircon age of the basement is ~ 2450 Ma [24]) tectonically juxtaposed with the Neoproterozoic island-arc and accretionary complexes [17, 26]. In many microcontinents, the lowermost parts of the section remain undated; in some, Archean and Paleoproterozoic rocks are unknown.

Neoproterozoic acid volcanics of elevated alkalinity or contrasting basalt–trachyrhyolite series are noted in many microcontinents. This are the Koksou Group of the Ulutau, the Qainar Formation of the Greater Qaratau, the formation of the Greater Naryn in the Chatkal–Naryn Block, the Altynsyngan Formation in the Aqtau–Moynty Massif, the Zabhan Formation in the Baydrag Massif, etc.

The origin of these volcanic rocks remains ambiguous; quite different genesis is ascribed to them. For example, as is suggested in [19, 25], all Precambrian microcontinents of the UMB initially belonged to the active margin of East Gondwana, and thus the acid and bimodal complexes are suprasubduction in nature. Other researchers suggest that they are related to rifting [3, 7, 39, 40].

In most microcontinents, the basement rocks are overlain with a stratigraphic or angular unconformity

by Upper Neoproterozoic–Lower Paleozoic terrigenous–cherty–carbonate cover. In most massifs (Ulu-tau, Lesser Qaratau, Zhungar, Aqtau–Moyynty), these complexes characterize the inner zone of the passive margin. They are characterized by compensated terrigenous–carbonate sediments of considerable thickness, phosphorite bodies in the lower part of the section, diverse benthic fauna, and a complete absence of metamorphism [7].

The similarity of the basement complexes and sedimentary covers in the sialic massifs of Central Kazakhstan and the North Tien Shan indicate that initially they made up the large Kazakh sialic domain with the Archean–Paleoproterozoic basement and the Upper Neoproterozoic–Cambrian cover [7, 40].

On the basis of approximately the same grounds, it can be supposed that the microcontinents currently situated to the south of Siberia (the Baydrag and Tarbogatay blocks, the Gargan Block as a constituent of the Tuva–Mongolian Massif, the Derbina–Arzybey and Sangilen microcontinents) also once made up a single sialic domain called Mongolian. These microcontinents are less studied than the sialic massifs of Central Kazakhstan and the North Tien Shan, and in this work we confine ourselves to demonstrating the similarity of the sections pertaining to the Baydrag, Tarbogatay, and Gargan blocks.

The hypothesis of the classification of these blocks as a single sialic massif is supported by several lines of reasoning. First is the similar U–Pb zircon age of the crystalline basement: 2646 ± 45 Ma for the Baydrag and Tarbogatay blocks [14] and ~ 2450 Ma for the Gargan Block [24]. Second, the last stage of progressive thermal metamorphism in all three blocks took place 1850–1800 Ma ago [40]. Third, the Neoproterozoic volcanic rocks of the Darkhot–Sarkhoy Group of the Tuva–Mongolian Massif are similar in age and composition to the volcanics of the Zabhan Formation of the Baydrag microcontinent. Finally, the terrigenous–carbonate covers of the Tuva–Mongolian Massif and the Baydrag microcontinent are comparable in composition, structure, and age. In both massifs, the lower part of the section consists of the tillite unit overlain by carbonate rocks (the Sabit Formation of the Hövsgöl Group of the Tuva–Mongolian Massif and the Tsagaan–Olom Formation of the Baydrag microcontinent). The similarity of these sections is emphasized repeatedly, e.g., in [2], and hardly requires detailed discussion. The above-listed facts allow us to put forward the hypothesis about the existence of the single Mongolian domain in the Neoproterozoic.

GEOLOGICAL POSITION OF THE SAMPLED SECTION

The Baydrag (Central Mongolian, Zabhan, Baydrag–Tarbogatay in other publications) Massif is situated in the western and northwestern part of the Han-

gay Highland. In the north, the massif borders along the Bolnay Fault on the Tuva–Mongolian Block and the Cambrian volcanic and sedimentary sequences of the Ider Belt. In the west and southwest, the massif borders on the Neoproterozoic–Cambrian island-arc complex of the Lake Zone, and in the east, on the narrow allochthon of the pre-Neoproterozoic Bayanhongor ophiolite complex and the Upper and Middle Paleozoic sedimentary sequences of the Central Hangay (Fig. 1b).

The basement complex of the Baydrag microcontinent is composed of tonalitic gneisses and enderbites of the Baydrag Group and metasedimentary rocks of the Bumburger Formation (Fig. 2). These rocks are cut through by the Paleoproterozoic granite with U–Pb zircon age of 1825 ± 5 Ma [16]. The latest episode of progressive thermal metamorphism took place 1850–1800 Ma ago [40]. In the east, these complexes are overlapped by thick terrigenous–carbonate sequence of the Olziit-Gol Formation presumably of Meso- or Neoproterozoic age.

The Neoproterozoic volcanic rocks of the Zabhan Formation that occurs largely in the southeastern part of the Baydrag microcontinent marks a separate stage of magmatic activity in the geological history of the microcontinent. The formation consists of basaltic andesite and andesite, which give way to acid volcanics upsection. The thickness of the formation exceeds 2000 m. The large amount of pyroclastic flows, ignimbrites, and other products of explosion volcanism confirm the subaerial character of the eruptions. This is supported by the locally developing conglomerate units, as well as by the thick red beds consisting of alluvial sandstone and siltstone of the continental molasse grading upsection into volcanic rocks.

The rocks of the Zabhan Formation underwent the Cadomian (Baikalian) Orogeny in the Late Precambrian. This is indicated by the folding, continental red molasse, and angular unconformity at the base of the Late Neoproterozoic sedimentary sequence.

In the basin of the Zabhan River, on the northern slope of the Khasagtyn–Nuruu Range, the Zabhan Formation is overlapped with a break in sedimentation and angular and stratigraphic unconformity by the Upper Neoproterozoic–Cambrian sedimentary group, which comprises from bottom to top the Tayshir Formation with tillites; dolomite and limestone of the Tsagaan–Olom Formation with phosphorites in the upper part of the section; terrigenous rocks of the Bayan-Gol Formation; and limestone of the Salany-Gol Formation. This group is dated sufficiently reliably from paleontological and chemostratigraphic data at the Upper Neoproterozoic–lowermost Cambrian [42].

The Salair orogenic phase is expressed in the Central Mongolian Massif in large-scale thrusting [42]. The complexes of the Late Neoproterozoic–Cambrian island-arc system were partly obducted on the

shelf of the microcontinent in the Late Cambrian and Ordovician. This is indicated by a large ophiolitic allochthon, whose fragments extend as a chain along the western margin of the microcontinent from the Mount Maikhan Uul in the south to the Onts Uul mountainous massif in the north. In the present-day structure, the shelf sedimentary rocks of the Tayshir, Tsagaan-Olom, Bayan-Gol, and Salany-Gol formations make up a packet of imbricate tectonic sheets [42].

The samples for paleomagnetic and geochronological studies were taken from the volcanic rocks of the Zabhan Formation in the valleys of the Tsagaan-Gol and Bayan-Gol rivers and near the Tayshir somon (Fig. 3); 29 pebbles were collected from intraformational conglomerate in the Bayan-Gol River valley.

In the studied sections, the volcanic rocks of the Zabhan Formation are composed of dacite, rhyodacite, and rhyolite (lavas, tuffs, and ignimbrites). These are largely relatively short lava flows and extrusions a few tens of meters in thickness. Dikes varying in thickness from 10 cm to a few meters are widespread.

GEOCHRONOLOGICAL DATA

Two samples were taken for geochronological study. Sample B66 was taken from a rhyolitic flow in the upper part of the section of the Zabhan Formation exposed along the Tsagaan-Gol River, whereas sample DZ-1 is from the lower part of this formation exposed along the Bayan-Gol River.

Zircons were separated by comminution, division of mineral fractions in heavy liquids, and electromagnetic separation. The least magnetic zircon grains were picked out by hand under a binocular microscope, placed into epoxy matrix with zircon grains of FC-1 standard, and polished. The isotopic measurements were carried out at the University of Florida using LA-MC-ICP-MS (laser ablation and measurement on a multicollector ICP mass spectrometer). A New Wave ultraviolet (213 nm) laser attached to a Nu Plasma ICP mass spectrometer was used for laser ablation of individual grains and measurement of the U and Pb isotope ratios. The equipment for the LA-MC-ICP-MS and analytical techniques are described in [84].

To take into account fractionation by evaporation of the sample under the effect of laser and mass discrimination of the mass spectrometer, the corresponding corrections were introduced into the measured U–Pb isotope ratios [45]. The uncertainties were estimated from the reproducibility of isotopic analysis of the reference FC-1 zircon [64], which was assigned to individual results. The $^{206}\text{Pb}/^{238}\text{U}$ ratios were corrected to common lead using the 207 method [89]. The $^{207}\text{Pb}/^{235}\text{U}$ ratios corrected to common lead were calculated from $^{238}\text{U}/^{235}\text{U} = 137.88$, the corrected $^{206}\text{Pb}/^{238}\text{U}$ ratio, and the normalized $^{207}\text{Pb}/^{206}\text{Pb}$ ratio. Traditional diagrams with concordia were drawn from these data with help of the Isoplot/Ex. v. 3.09a [56].

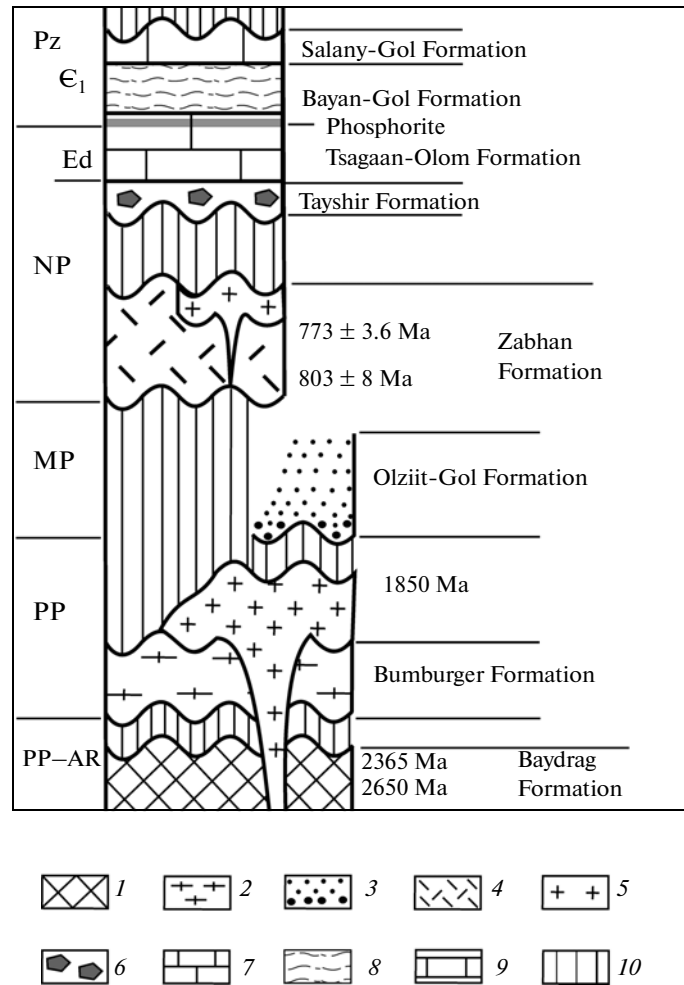


Fig. 2. Schematic stratigraphic column of the Baydrag microcontinent. (1) Tonalitic gneiss of the Baydrag Formation; (2) gneiss, marble, and quartzite of the Bumburger Formation; (3) graywacke of the Olziit-Gol Formation; (4) rhyolite, dacite, and andesite of the Zabhan Formation; (5) granite; (6) tillite of the Tayshir Formation; (7) limestone and dolomite of the Tsagaan-Olom Formation; (8) sandstone, siltstone, and claystone of the Bayan-Gol Formation; (9) limestone of the Salany-Gol Formation; (10) hiatus in section.

Samples B66 and DZ-1 contain zircons with concordant U–Pb ages (Fig. 4; Table 1). Six subhedral zircon grains 150–200 μm in size yielded a concordant age of 773.5 ± 3.6 Ma; MSWD = 0.5 (Fig. 4a). Four zircon grains from sample DZ-1 were measured; one grain yielded a concordant age of ~1085 Ma, whereas the three other grains gave 803.4 ± 8.0 Ma; MSWD = 0.1 (Fig. 4b). These data estimate the age interval of the Zabhan Formation at 805–770 Ma. The age of 1085 Ma obtained for one grain probably reflects contamination of volcanic rocks by basement material.

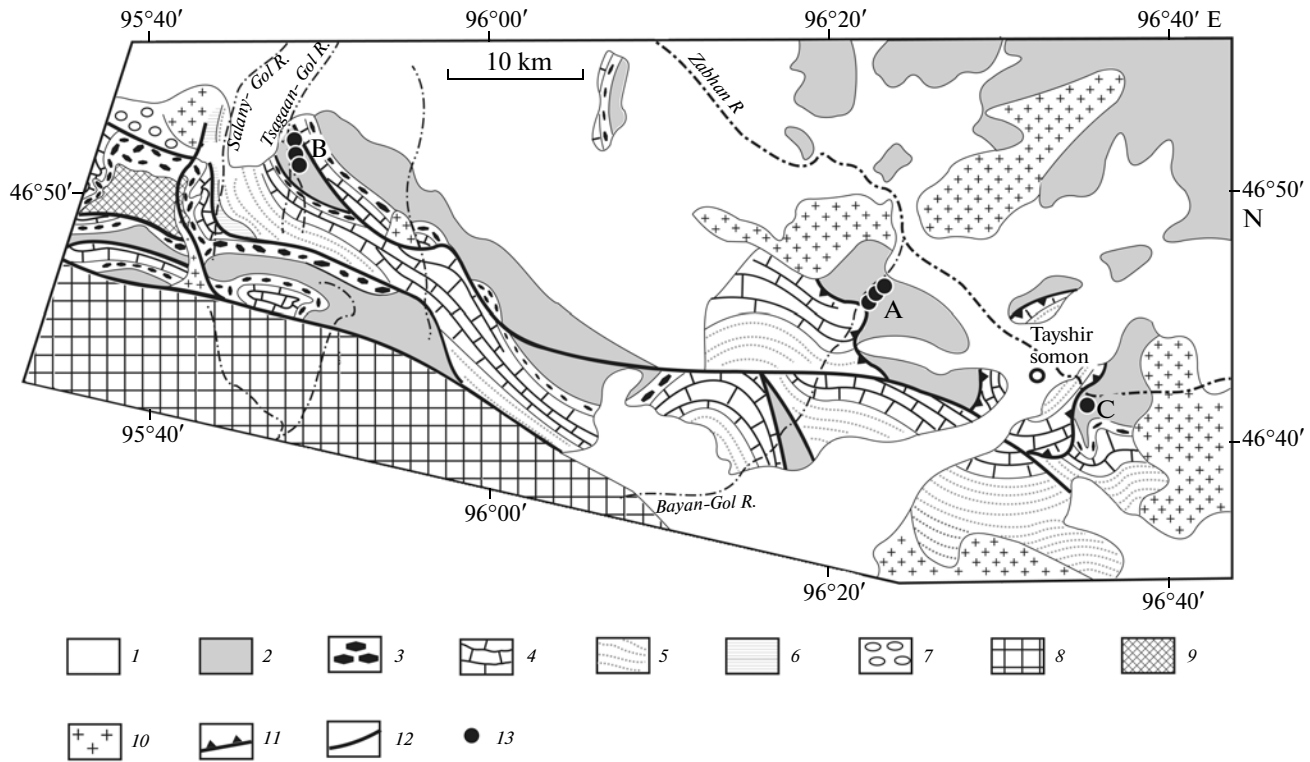


Fig. 3. Geological scheme of the Khasagtyn-Nuruu Range, West Mongolia. (1) Cenozoic sediments; (2) Zabhan Formation; (3) Tayshir Formation; (4) Tsagaan-Olom Formation; (5) Bayan-Gol Formation; (6) Salany-Gol Formation; (7) Ordovician conglomerate; (8) Upper Neoproterozoic–Cambrian sequences of the Lake Zone; (9) serpentinitized ultramafic rocks; (10) Paleozoic granitoids; (11) thrust fault; (12) strike-slip fault; (13) areas of sampling. Letters in figures: A, area of sampling in the Bayan-Gol Valley; B, area of sampling in the Tsagaan-Gol Valley; C, section near Tayshir somon.

PALEOMAGNETIC DATA

Research Technique

The samples were collected from outcrops either by hand, with their orientation measured with a magnetic compass, or using a portable drill and measuring the orientation of the cores with a solar compass. The samples were grouped into sites, each site corresponding to a lava flow. Cubes with edge of 20 mm were sawed out from hand samples and cylinders 22 mm in length from the cores. The sample collections were studied at the paleomagnetic laboratories of the Geological Institute, Russian Academy of Sciences in Moscow and the University of Florida in Gainesville. All samples underwent stepwise (up to 20 steps) thermal demagnetization up to 680°C. In Moscow, this procedure was conducted in a custom-made furnace with a two-layer permalloy screen and a residual field of ~10 nT. Magnetization was measured on a JR-4 spinner magnetometer with a noise level of 0.05 mA/m placed into Helmholtz coils to decrease the effect of the terrestrial magnetic fields by several tens of times. In Gainesville, stepwise thermal cleaning was carried out in an Analytical Services TD-48 furnace; magnetization was measured on a 2G Enterprises cryogenic

magnetometer. Both the furnace and magnetometer were placed into a nonmagnetic room.

The results of heating were presented as orthogonal diagrams [94]. To determine the directions of the magnetization components, linear segments of the path, which included no less than three measurements, were used [44]. The data on the samples from one flow were averaged and the mean vectors for the flows (sites) were used for calculation of the mean direction for the entire sequence. In those sites where magnetization components were not isolated in all samples, the site-mean directions were calculated by combining magnetization components and remagnetization circles [59]. The data were processed with software by J.-P. Cogné [30], R. Enkin, and S.V. Shipunov.

Results

In most samples of volcanic rocks from the Zabhan Formation, low-temperature magnetization component A directed along the present-day field is removed at a temperature of 300–350°C (Figs. 5a, 5b). Most likely, this is viscous magnetization. Because this component does not bear useful information, it is not con-

sidered below and the NRM directions are not shown in the orthogonal diagrams [94].

After removal of component A, medium-temperature component B was established in 18 of 21 sites (Figs. 5a–5d; Table 2). This component is removed in the temperature interval of 480 to 575°C. This component is well grouped within each site (Table 2) both in geographic and stratigraphic coordinates. The best grouping of mean directions by sites is achieved in the geographic coordinate system Dec = 273°, Inc = –66°, k = 19, and a95 = 8.2° (Fig. 6a).

After removal of component B, a high-temperature component C that shows the rectilinear decay to the origin was isolated in 11 of 21 sites (Figs. 5a–5c; Table 3). When we could not isolate different components, the site-mean directions were computed by combining component directions and remagnetization circles [59]. Component C is well grouped in all sites (Table 3); the best grouping of mean directions by sites is achieved in the stratigraphic coordinate system: Dec = 322°, Inc = –65°, k = 19, and a95 = 10.7° (Fig. 6d); the fold test [58] is positive. The mean direction obtained for one of the sites is approximately antipodal to the other ten sites (Fig. 6d).

It should be noted that the distributions of the mean directions by sites for components B and C are partly overlapped, especially in the stratigraphic system of coordinates. As a result, we are not always sure as to the primary or secondary nature of certain components. This situation is, for example, characteristic of sites N4175 and N4306, where the primary and secondary mean-directions look rather similar. At the same time, it is clearly seen in the orthogonal diagrams that these are distinct components (Fig. 5d). With a high degree of probability it can be asserted that the partial overlapping of the distribution is accidental, so that the magnetization components can be isolated quite reliably.

In some samples, the blocking temperatures are below 580°C, but in most cases they reach 670–675°C (Fig. 5). Magnetite and hematite occurring in variable proportions probably are carriers of magnetization in the studied rocks.

In 16 of 29 pebbles taken from the intraformational conglomerate, both medium- and high-temperature components can be isolated (Fig. 5d). In the rest of the pebbles, only one component, which does not decay to the origin, is recognized. The direction of the medium-temperature component coincides with the direction of component B in the host rocks. The directions of the high-temperature component isolated from 16 pebbles are chaotic (Fig. 6e), and the value of the normalized resultant vector is 0.20; i.e., much lower than the 95% critical value equal to 0.40 [57]; in other words, the conglomerate test is positive.

We failed to isolate high-temperature component C in 10 of the 21 sampled sites. In the lava samples from

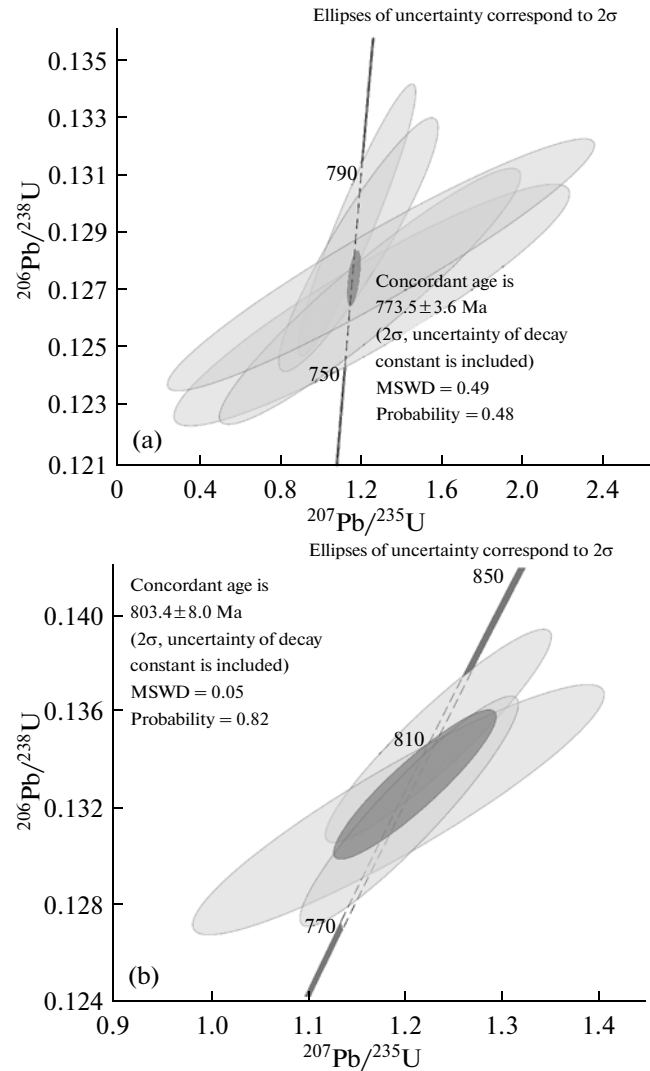


Fig. 4. Diagrams with concordia for (a) sample B66 (upper part of the Zabhan Formation) and (b) sample DZ-1 (lower part of the Zabhan Formation).

sites J2, J8, N4047, and N4214 we isolate only one component, which does not decay to the origin (Fig. 5f). In the samples from sites J11, J6, and J7, only one that decay to the origin is recognized (Fig. 5g), but its direction coincides with the direction of component B in the other sites and with the direction of the medium-temperature component in the conglomerate (Fig. 6a).

Having combined the directions of component B in the two-component samples; the direction of remagnetization in the conglomerate; the directions of component B in sites J2, J8, N4047, and N4214; and the high-temperature directions in sites J6, J7, and J11, we see that the best grouping of mean directions by sites is achieved in the geographic system of coordinates (Fig. 6a); the fold test is negative. Thus, component B (pole 31N, 147E) is undoubtedly secondary

Table 1. La-ICP-MS data on volcanic rocks of the Zabhan Formation

Zircon grain	$^{207}\text{Pb}/^{235}\text{U}$	1 σ	$^{206}\text{Pb}/^{238}\text{U}$	1 σ	$^{207}\text{Pb}/^{235}\text{U}$ age	1 σ	$^{206}\text{Pb}/^{238}\text{U}$ age	1 σ	% Discordance
B66-4	1.16465	0.11778	0.12957	0.00194	784	54	785	11	0
B66-6	1.23796	0.39719	0.12660	0.00173	818	166	768	10	6
B66-13	1.17473	0.02715	0.12920	0.00201	789	13	783	11	1
B66-15	1.17153	0.16057	0.12871	0.00181	787	72	781	10	1
B66-16	1.22852	0.30248	0.12690	0.00183	814	129	770	10	5
B66-17	1.28073	0.42896	0.12801	0.00180	837	175	776	10	8
DZ-1	1.20556	0.04637	0.13176	0.00197	803	21	798	11	1
DZ-2	1.19456	0.08735	0.13183	0.00214	798	40	798	12	0
DZ-6	1.23607	0.04803	0.13492	0.00183	817	22	816	10	0

Notes: Samples B66-4 and DZ-1 were taken from a rhyolitic flow in the upper and lower parts of the section, respectively; 1 σ is the uncertainty of individual ratios and calculated ages; discordance is the difference between the $^{207}\text{Pb}/^{235}\text{U}$ and $^{208}\text{Pb}/^{238}\text{U}$ values expressed in percent.

Table 2. Mean directions of component B in volcanic rocks of the Zabhan Formation

S	N/N ₀	B	Present-day coordinate system				Past coordinate system			
			D°	I°	k	a ₉₅ ^o	D°	I°	k	a ₉₅ ^o
N4047	7/7	326/90	229.6	-66.7			169.1	2.5	199	4.3
N4055	5/8	326/90	296.4	-43.8			173.2	-38.9	42	11.9
N4063	6/8	326/90	236.2	-73.9			162.1	-0.1	34	3.6
J1	7/7	326/90	248.8	-76.7			159.0	-2.9	114	5.7
J2	12/12	326/90	230.3	-72.7			163.2	1.7	54	5.9
J3	8/9	326/90	280.2	-84.0			150.3	-4.2	222	3.7
J5	4/7	326/90	287.6	-83.6			150.0	-5.0	262	5.7
J6	11/12	326/90	230.7	-72.5			163.5	1.6	65	5.7
J7	6/7	326/90	235.8	-71.5			164.6	0.1	132	5.8
J8	8/9	326/90	265.5	-84.6			150.7	-2.6	76	6.4
J11	11/15	225/40	263.8	-63.0			181.4	-59.4	27	8.6
N4175	5/7	267/37	276.0	-48.7			323.8	-82.9	83	8.7
N4190	5/8	267/37	286.8	-35.7			313.7	-67.8	41	12.2
N4206	5/7	267/37	286.6	-40.8			322.3	-72.0	47	11.3
N4214	8/8	267/37	267.8	-72.1			86.3	-70.9	44	8.4
N4252	5/7	267/37	310.8	-46.3			1.4	-61.3	31	13.9
N4260	6/8	267/37	279.2	-53.4			5.0	-82.7	106	6.5
Conglomerate	23/29	267/37	271.8	-63.8			75.9	-78.9	15	8.0
MEAN	(18/21)		272.8	-66.2	19	8.2	158.7	-42.8	3	24.7

Notes: S, site of sampling; MEAN, overall mean direction; N/N₀ is the ratio of number of samples used for analysis to the number of samples taken in each site; B, mean azimuth of dip/dip angle; D, declination; I, inclination; k, concentration parameter; a₉₅ radius of confidence circle [33].

and was acquired after the Late Cambrian–Early Ordovician deformations. The exact age of component B can hardly be established. It is noteworthy,

however, that the rocks of the Baydrag Block are cut through by several Early Permian intrusions, which also occur in the sampled area. In the completely

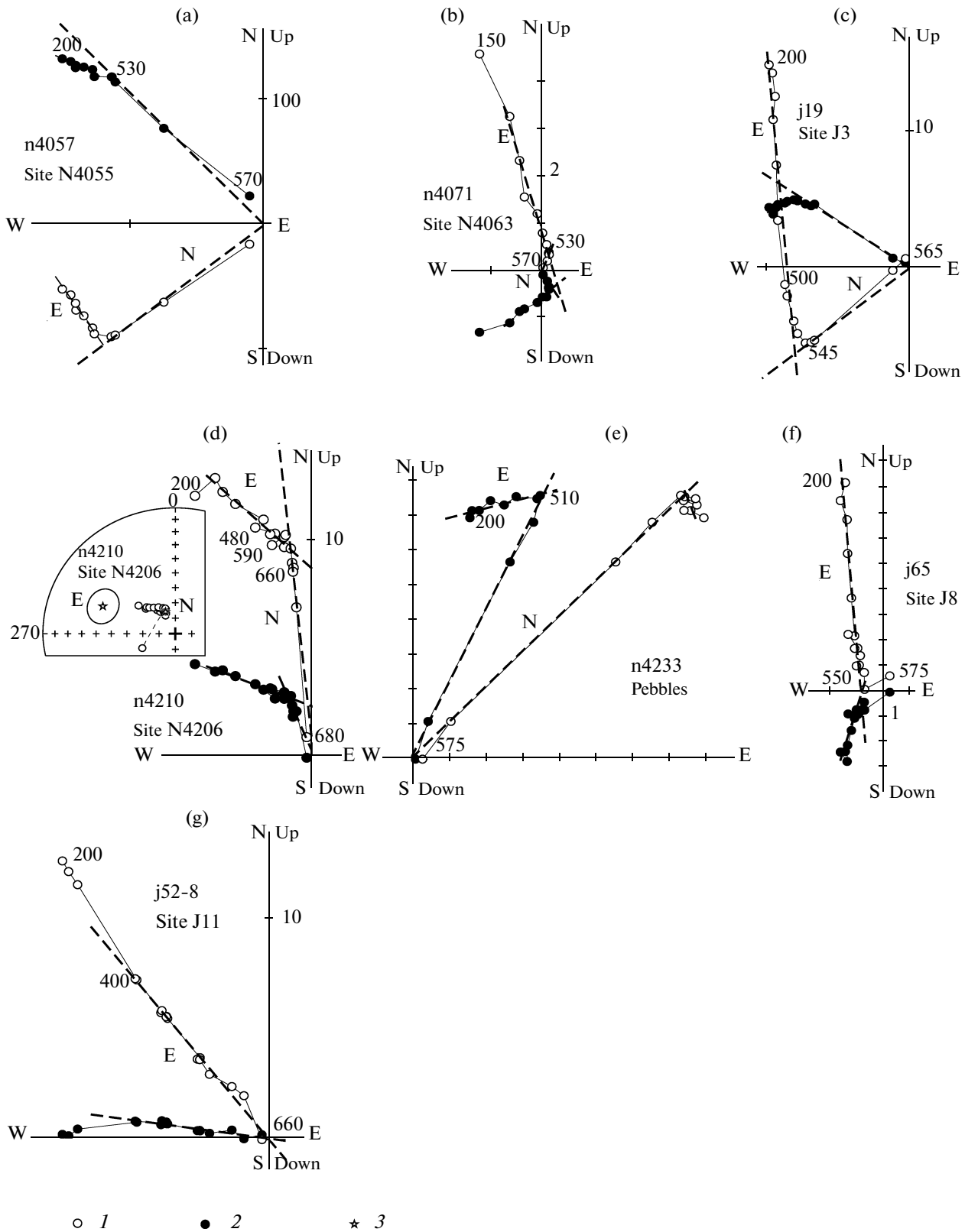
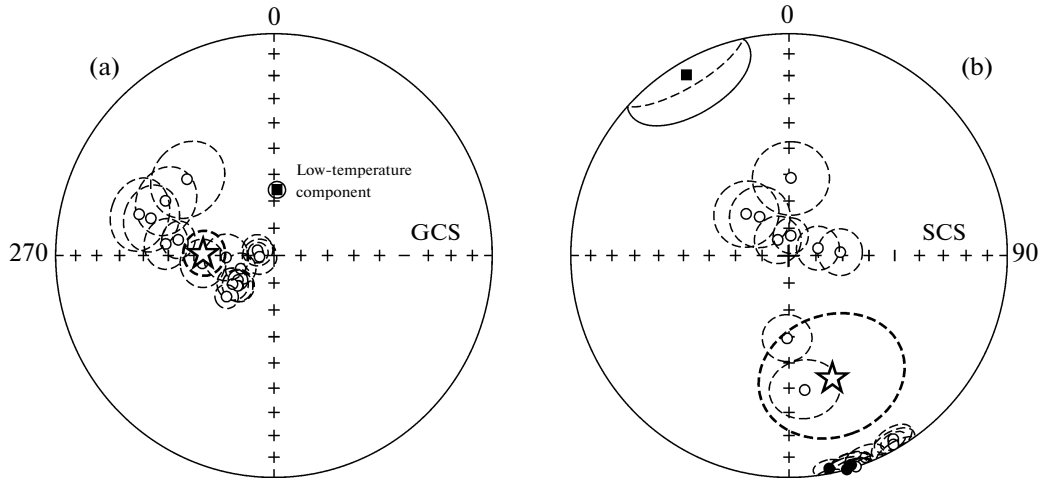
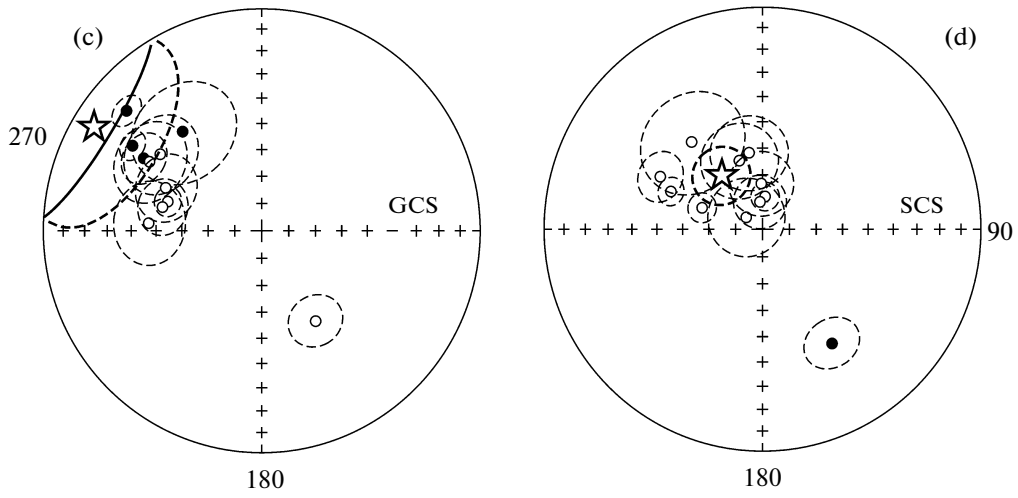


Fig. 5. Examples of the Zijderveld's diagrams for volcanic rocks of the Zabhan Formation: (a–d, f, g) dacite and rhyolite flows; (e) pebbles from intraformational conglomerate. All diagrams are given in the past coordinate system; temperature is expressed in C and magnetization in mA/m. In the stereogram all symbols are projected on the upper hemisphere. (1) Projection on horizontal plane; (2) projection on vertical plane; (3) directions of separate components.

Medium-temperature component B



High-temperature component C



High-temperature component C in pebbles

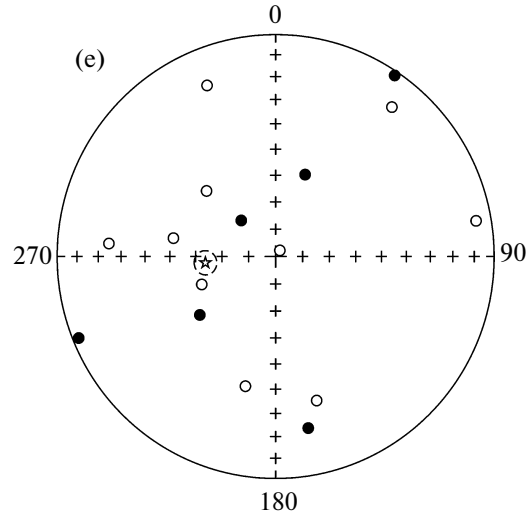


Fig. 6. Stereograms of the mean-site magnetization directions for volcanic rocks of the Zabhan Formation. Dots are mean-site magnetization directions with confidence circles (dashed lines) in (a, b) geographic (GCS) and (c, d) stratigraphic (SCS) coordinate systems. The medium-temperature magnetization component is shown in (a, b) and high-temperature magnetization component, in (c, d); (e) direction of high-temperature magnetization component for pebbles from intraformational conglomerate. Stars are overall mean components with confidence circles (heavy dashed lines). Open symbols and dashed lines are projected on the upper hemisphere; filled symbols and solid lines are projected on the lower hemisphere.

remagnetized lavas of site J11 sampled near one such intrusion, the attributes of contact metamorphism are documented. It can be suggested rather reliably that component B is Early Permian in age.

Conversely, component C is most likely primary. This is confirmed by the positive fold test, pebble test in the intraformational conglomerate, and also by the fact that 1 of the 11 mean directions by sites is approximately antipodal to the others (Fig. 6d). The mean inclination $65 \pm 11^\circ$ corresponds to the paleolatitude of $47 \pm 14^\circ$. Thus, 805–770 Ma ago, the Baydrag microcontinent was situated at a latitude $47 \pm 14^\circ$ N or S.

DISCUSSION

The concept of the Rodinia supercontinent that originated 1300–1100 Ma ago and broke down 800–700 Ma ago is currently popular [52]. After the breakdown of this supercontinent, its fragments in the form of continental blocks migrated towards opposite sides of the Earth to make up a new supercontinent called Gondwana. West Gondwana was formed almost completely as early as 600 Ma ago, whereas Australia, East Antarctica, India, East Africa, and the Kalahari remained separated by large oceanic basins [68]. Gondwana was eventually formed approximately 540–530 Ma ago, when India collided with Australia and East Antarctica along the Kuunga Orogen [68].

The breakdown of Rodinia and the formation of Gondwana are known only in approximate terms. The available paleomagnetic data are not sufficient to restore the kinematics of even the largest plates in this time interval. Much less is known about the kinematics of such relatively small domains as, for example, the Mongolian or Kazakh domains.

Origin of Precambrian Sialic Massifs of the Ural–Mongolian Belt

Most hypotheses on the origin of microcontinents in the UMB, e.g., [11, 19, 41], are based largely on the lithologic similarity of the Upper Neoproterozoic–Lower Paleozoic sections of the microcontinents with coeval sections of the Tarim, South China, and Siberian platforms [9, 15]. The closeness of the stratigraphic and paleontological data concerning these sections has allowed different authors to develop alternative models. Thus, Berzin and Dobretsov [28] suggested that most microcontinents are Siberian in origin, whereas other authors, e.g., [19, 41], concluded that all these blocks had broken off from East Gondwana. Khain et al. [40] put forward the hypothesis that all Kazakh microcontinents initially were parts of the Tarim Platform.

New geochronological and paleomagnetic data allow us to revisit this issue. To date, paleomagnetic

Table 3. Mean directions of component C in volcanic rocks of the Zabhan Formation

S	N/N ₀	B	Geographic coordinate system				Stratigraphic coordinate system			
			D°	I°	k	a ₉₅	D°	I°	k	a ₉₅
N4055	8/8	326/90	311.1	18.9			289.2	−66.1	107	5.4
N4063	7/10	326/90	148.8	−50.6			148.3	39.3	39	9.8
J1	7/7	326/90	301.1	37.0			296.8	−46.5	50	8.8
J3	8/9	326/90	302.9	30.2			292.0	−52.7	129	5.0
J4	7/9	326/90	321.0	42.0			320.5	−47.8	12	19.1
N4175	6/7	267/37	273.8	−47.0			305.6	−82.6	23	14.4
N4190	8/8	267/37	301.2	−39.7			341.1	−63.3	18	14.2
N4198	6/8	267/37	287.0	−52.9			4.6	−78.0	170	5.3
N4206	3/7	267/37	293.7	−50.3			358.4	−73.3	147	12.0
N4252	5/7	267/37	306.6	−41.7			349.9	−61.3	39	14.1
N4260	6/8	267/37	283.2	−51.4			354.6	−80.0	49	9.0
MEAN	(11/21)		311.7	−11.0	3	30.1	321.9	−65.0	19	10.7

Note: See Table 2 for abbreviations.

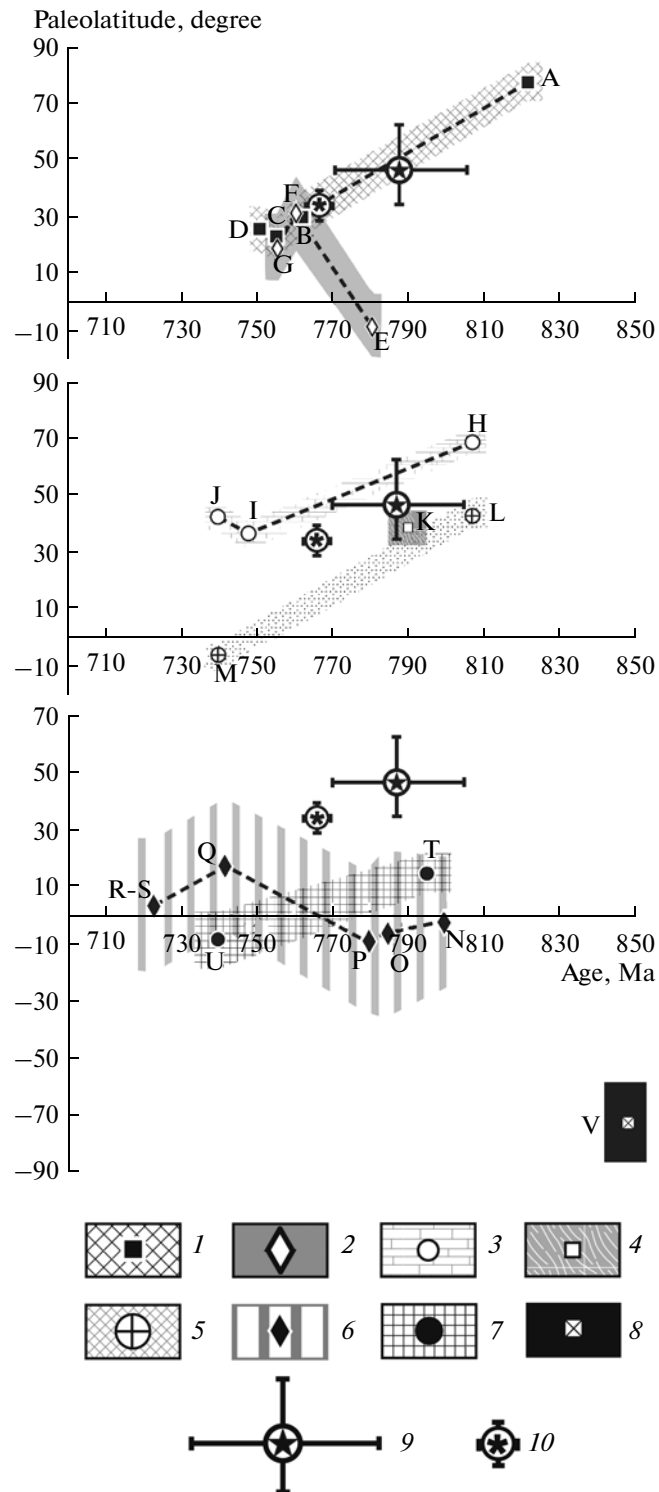


Fig. 7. Paleolatitude versus age of main cratons listed in Table 4. The position of the central part of each craton is shown by symbols; the latitudinal interval occupied by each craton (without confidence intervals) is shown by a band. If a craton has more than two poles in the considered time interval, the symbols are connected by heavy dashed line. (1) India; (2) Australia; (3) South China; (4) North China; (5) Tarim Platform; (6) Laurentia; (7) Siberia; (8) Baltica; (9) paleolatitude determined for the Zabhan Formation of the Baydrag microcontinent; (10) paleolatitude determined for the Qurgan Formation of the Lesser Qaratau microcontinent. The results for microcontinents are shown with confidence intervals.

Table 4. Selected paleomagnetic poles for the main platforms

Object	Age, Ma	Pole		A_{95} , degree	Latitudes	Reference
		(N°)	(E°)			
India						
Harohalli Dikes (A)	821 ± 12	27	79	9	85–71N	[73]
Malani Rhyolite, India (B)	761 ± 10	75	71	10	39–23N	[82]
Mahe Granite, Seyshelles ^c (C)	755 ± 1	77	23	2	32–15N	[83]
Mahe Dikes, Seyshelles ^c (D)	750 ± 3	80	79	16	34–18N	[34, 83]
Australia						
Hussar Formation (E)	800–760	62	86	10	3–19S	[70]
Mundine Dikes (F)	755 ± 3	45	135	4	31–8N	[90]
Walsh Tillite (G)	750–770	22	102	14	44–19N	[49]
Yaltipena Formation ^c	620–630	44	173	8	27–5N	[78]
Elatina Formation ^c	600–620	39	186	9	26–1N	[78]
Brachina Formation ^c	~580	33	148	16	44–20N	[60]
Lower Arumbera/Pertataka Formation ^c	~570	44	162	10	30–7N	[43]
Lower Arumbera ^c	~550	46	157	4	30–6N	[43]
Todd River	~530	43	160	7	32–9N	[43]
South China						
Xiaofeng Dikes (H)	807 ± 10	14	91	11	~69N	[51]
Liantuo Formation (I)	748 ± 12	4	161	13	~37N	[32]
Natuo Formation ^d (J)	~740	0	151	5	~43N	[74]
Meishucun Formation ^d	~525	9	31	10	~14N	[53]
Tianheban Formation ^d	~511	–7	10	23	~12S	[53]
Hetang Formation ^d	~511	–38	16	17	~18S	[53]
North China						
Nanfen Formation (K)	800–780	–16	121	11	~39N	[93]
Mean pole	~700	–43	107	6	~11N	[93]
Donjia Formation	~650	–61	97	7	~8S	[93]
Tarim						
Aksu Dikes (L)	807 ± 12	19	128	6	~43N	[29]
Baiyixi Formation	~740	17	194	4	6S	[37, 41]
Laurentia						
Galeros Formation (N)	780–820	–2	163	6	21N–25S	[88]
Wyoming Dikes (O)	782 ± 8	13	131	4	23N–36S	[35]
Tsezotene Sills and Dikes (P)	779 ± 2	2	138	5	16N–34S	[66]
Kwagunt Formation (Q)	742 ± 6	18	166	7	41N–6S	[88]
Natkusiak Formation (R)	723 ± 4/–2	6	159	6	27N–20S	[36, 65]
Franklin Dikes (S)	723 ± 4/–2	5	163	5	27N–19S	[36, 67]
Long Range Dikes ^a	620–610	19	355	18	34N–6S	[63]
Callander Complex	575 ± 5	–46	121	6	34–81S	[80]
Catochin A Basalt	564 ± 9	–42	117	9	32–77S	[61]
Sept-Iles B Complex ^b	564 ± 4	–44	135	5	27–74S	[81]

Table 4. (Contd.)

Object	Age, Ma	Pole		A_{95} , degree	Latitudes	Reference
		(N°)	(E°)			
Siberia						
Karagas Group (T)	850(?)–740	–12	97	10	22–8N	[18, 68]
Nersa Complex (U)	~740	–37	122	11	2N–19S	[18, 68]
Mean pole for Ediacaran	~560	–35	77	6	3–16S	[76]
Redkolesny Formation	~550	–61	68	5	30–42S	[76]
Mean pole for Nemakit–Daldyn time	~540	–60	115	7	25–41S	[68]
Mean pole for Early Cambrian	~525	–48	151	8	19–36S	[68]
Baltica						
Hunnedalen Dikes (V)	~848	–41	222	10	59–87S	[85]
Egersund Dikes	~608	–31	224	15	50–81S	[86]
Mean pole	~555	–30	298	10	4–31S	[38, 71, 72]
Tornetrask Formation	~535	–56	296	12	24–52S	[82]

Notes: The latitudes are the interval of originating latitudes. Letters in parentheses after names of objects are their notations in Fig. 7.

^a Recalculated after Hodych et al. (2004).

^b Direction B of the Sept-Iles Complex after correction for deformation [80] coincides with other poles ~570 Ma in age for Laurentia, whereas direction A coincides with the Cambrian–Ordovician segment of the curve of apparent pole wandering for North America, after Meert and Van der Voo (2001).

^c Approximate age based on stratigraphic information [69] and the scale of variation of isotopic composition [87].

^d Approximate ages based on stratigraphic position of section and/or isotopic data.

^e Rotated relative to India, after [83].

data are available only for two microcontinents in the UMB: the Lesser Qaratau Block in Central Kazakhstan, which probably can be regarded as a part of the Kazakh sialic domain [48], and the Baydrag Block in Central Mongolia as a probable part of the Mongolian sialic domain (this paper). According to these data, 805–770 Ma ago the Baydrag Block (Mongolian sialic domain) was situated at a latitude of $47 \pm 14^\circ$ N or S, whereas the Lesser Qaratau Block (Kazakh sialic domain) 766 \pm 3.6 Ma ago was located at a latitude of $34.2 \pm 5.3^\circ$ N or S.

The age of the rocks studied in the Baydrag and the Lesser Qaratau blocks approximately corresponds to the very beginning of the breakdown of Rodinia. No single viewpoint on the position of the various cratonic blocks that made up Rodinia currently exists. Therefore, we compared the paleolatitudes estimated for the Baydrag and Lesser Qaratau blocks with the position of the major cratonic blocks within Rodinia, rather than with this supercontinent as a whole (Fig. 7; Table 4).

The polarity of the paleomagnetic determinations obtained for the Baydrag and Lesser Qaratau blocks cannot be established; i.e., the microcontinents in the Neoproterozoic could have been located either in the Northern or Southern hemispheres. If the microcontinents were in the Southern hemisphere, they should

have been located near the West Gondwana cratons: West Africa and Amazonia or amidst the Brazilian ocean. If the microcontinents were in the Northern hemisphere, they could have belonged to one of the North Rodinian plates: India, Australia, Tarim, or North or South China (Fig. 7; Table 4). Laurentia and Siberia were situated much further south (Table 4).

According to paleontological data and paleobiogeographic reconstructions, the microcontinents of the UMB were located in the Early Cambrian near Siberia, Australia, Tarim, and South and North China [9, 10, 21]. Thus, if in the Late Neoproterozoic the microcontinents were situated in the Northern hemisphere, their pathway to the Late Neoproterozoic–Cambrian location was much shorter and simpler than if they had to travel toward Siberia from West Africa or Amazonia. Thus, we suggest that at the end of the Neoproterozoic, the microcontinents of the UMB belonged to one of the North Rodinian plates.

The existence of the Paleoproterozoic basement and igneous complexes coeval with the Zabhan Formation of the Baydrag microcontinent and the Qurgan Formation of the Lesser Qaratau is an additional piece of evidence that could help us to constrain the possible parental plates. Paleoproterozoic basement can be found in any of the aforementioned plates. At the same

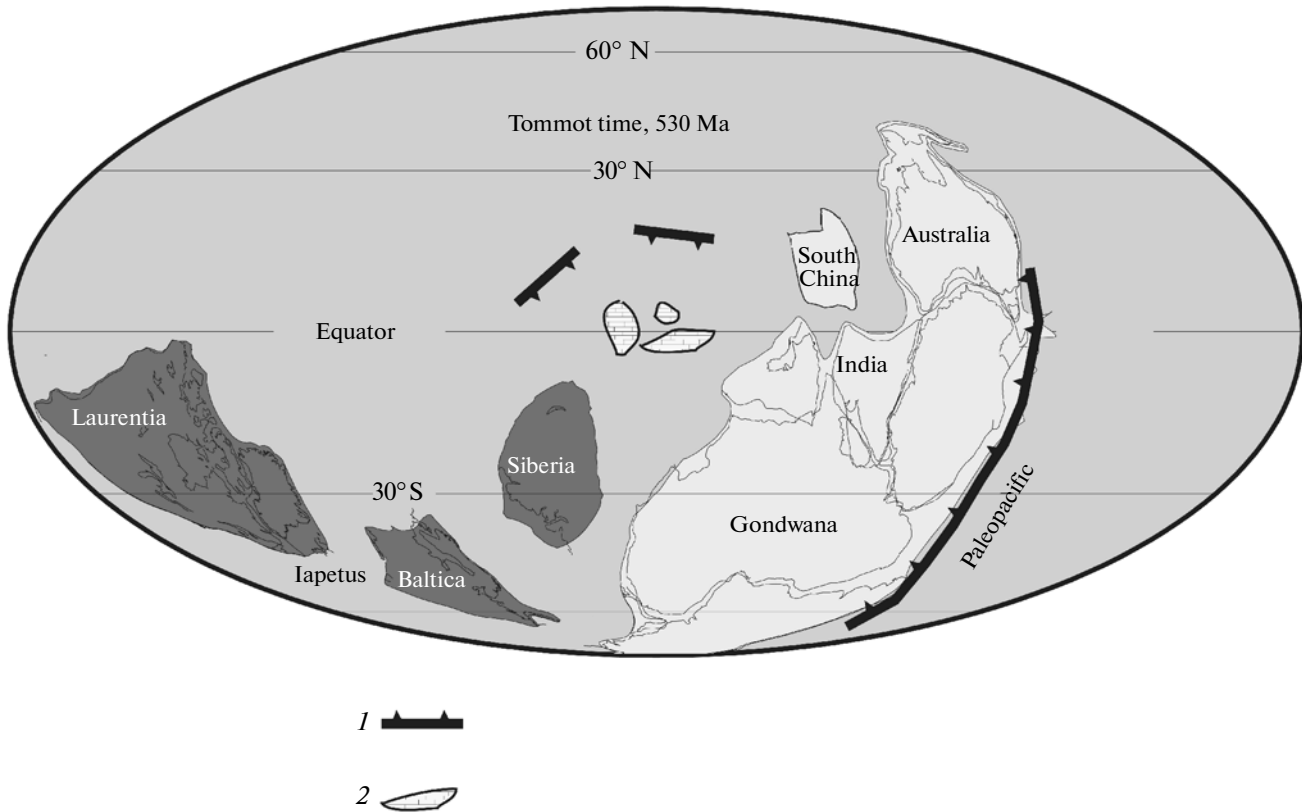


Fig. 8. Paleogeographic reconstruction for the Tommot time demonstrating presumable position of microcontinents of the Ural–Mongolian Belt and active island arcs. The continents of the Gondwana Group are light while the continents that do not belong to Gondwana are dark. (1) Subduction zone; (2) blocks with terrigenous–carbonate cover.

time, no igneous rocks dated at 1100–700 Ma are known in North China [55], which can be ruled out from consideration. In Australia, igneous rocks 800–750 Ma in age are rare and develop only locally [84], and this makes it hardly probable that the microcontinents belong to Australia. To choose between India, Tarim, and South China is not so simple. Anorogenic bimodal magmatism 860–730 Ma in age is well-known in India [27]. The Malani volcanic province and the volcanic rocks in the islands of the Seychelles are dated at ~777 Ma [82, 83]. In Tarim, rift-related volcanics are widespread, including bimodal series similar to the Zabhan Formation in composition; they are dated at 820 to 740 Ma [54]. Rift-related bimodal volcanism dated at 830–795 and 780–745 Ma is rather widespread in South China [50].

The most probable scenario is that in the Neoproterozoic the Baydrag and Lesser Qaratau blocks belonged to India, Tarim, or South China. If it is valid that these blocks are parts of the larger Mongolian and Kazakh sialic domains, our conclusion can be spread over two domains as large as Madagascar in size.

Probable History of Travel of the Mongolian and Kazakh Sialic Domains in the Late Neoproterozoic and Early Paleozoic

As was suggested above, before the breakdown of Rodinia, the Mongolian and Kazakh domains belonged to one of the North Rodinian plates. However, one can only guess when these domains were detached from the parental plate and how they traveled 750–550 Ma ago. In our reasoning we mainly rely on the same stratigraphic, lithologic, and paleontological data as the authors of the known models of evolution of the UMB [9, 11, 15, 19, 28, 40, 41]. Nevertheless, we consider it worthwhile to set forth here our view on the subsequent history of the Mongolian and Kazakh domains.

For most microcontinents of the UMB, geological records for the time interval of 750 to 600 Ma are either absent completely or remain very fragmentary [14]. As a rule, the Neoproterozoic is followed by a break in sedimentation up to 200 Ma long, i.e., up to the formation of the sedimentary cover. Evidence for such a break in almost all blocks compels us to suggest that they occurred at that time under similar conditions. The long hiatus most likely corresponded to the emergence above sea level, and this is more plausible

for a large domain rather than for many small islands. It can be supposed that 750–600 Ma ago microcontinents of the UMB remained still undetached from the parental plate or belonged to one or two large massifs, for example, to the Mongolian and Kazakh domains.

At the end of the Neoproterozoic the hiatus terminated, and terrigenous–carbonate cover started to deposit. The structure and composition of the cover's sections are similar to many microcontinents. In particular, the same unit of Upper Neoproterozoic glacial diamictites and phosphorites at the bottom of the Cambrian sequence is described from most sections [13]. The Tsagaan-Olom Formation of the Baydrag microcontinent, the Hövsgöl Group of the Tuva–Mongolian Massif, the Bokson Group of the Eastern Sayan, the Qapal and Basaga formations of the Aqtau–Zhungar Massif, and the Tamdy Group of the Lesser Qaratau are examples. Sections similar in structure and composition deposited at the same time in Tarim, South China, and South Siberia [44 and references therein].

The available geological data allow us to suggest that at the end of the Neoproterozoic and in the Early Cambrian a shallow-water basin with an archipelago of continental blocks existed near the Siberian Platform (Fig. 8) and even to describe some features of this hypothetical basin.

(1) Widespread carbonate rocks and a single paleomagnetic result on the Upper Neoproterozoic–Cambrian sedimentary complexes of the UMB (Baydrag Block [46]) indicate that the basin was situated at equatorial latitudes.

(2) In all coeval terrigenous–carbonate sections of microcontinents in the UMB, Tarim, South China, and South Siberia, the small-shell fauna of the Nemaikit–Daldyn and Tommot ages (542–520 Ma) has many common taxons at the levels of families, genera, and even species [9]. According to Repina [21], the benthic trilobite fauna of the Atdaban and Bottom times found in these sections belonged to the same Altai–Sayan paleobiogeographic province. It is noteworthy that the small-shell fauna which appeared in Siberia at the early Nemaikit–Daldyn time is also known in the Tommot sequences of many microcontinents of the UMB and in the Atdaban rocks of Australia [9]. The same can be said about archaeocyathids. The first archaeocyathid reefs appeared in Siberia at the onset of the Tommot time and reached Australia only in the middle Atdaban time [10]. It can be suggested that the habitat of this fauna in a hypothetical basin that widened from Siberia to the Mongolian and Kazakh massifs, Tarim, and South China, and then toward Australia.

(3) The lithology and geochemistry of the terrigenous rocks from the complexes of the Upper Neoproterozoic–Cambrian cover of the composite Tuva–Mongolian Massif show that the plagiogneisses and plagiogranites of the Gargan Block along with the

Neoproterozoic ophiolites and island-arc complexes were the main provenance of clastic material [5]. No indications of supply of clastic material from the Early Precambrian basement of the Siberian Platform are established. In the Late Neoproterozoic–Early Cambrian, the composite Tuva–Mongolian Massif was probably separated from the Siberian Platform by a marine basin. Most likely the sialic domains with microcontinents of the UMB were also separated from large cratonic blocks by relatively wide marine basins.

(4) Late Neoproterozoic–Early Cambrian island-arc complexes are well known in various parts of the UMB, including those near the Precambrian sialic blocks. Ruzhentsev and Burashnikov [22] and Gibsher et al. [6] described the island arc-complexes of this age in the Lake Zone of West Mongolia (Fig. 1b) and suggested that this island-arc system is traced toward Southeast Tuva. The Selety and Bozshakol–Chingiz island arcs arose in the Early Cambrian in North and East Kazakhstan, respectively. Fragments of the Early Cambrian island-arc complexes are known in South Kazakhstan as well [7]. At the same time, no tuffaceous admixture is found in the sedimentary covers of the microcontinents [23]. It is suggested that in the Late Neoproterozoic–Early Cambrian, the island arcs in the hypothetical basin were located at a significant distance from the sialic massifs.

CONCLUSIONS

At present, we are not ready to offer a fair model of the evolution of the Ural-Mongolian Mobile Belt in the Late Neoproterozoic–Early Cambrian. We can only list a number of facts necessary to keep in mind for substantiation of such a model and set forth several hypotheses differing in degree of proof.

(1) It can be suggested that in the Late Neoproterozoic–Early Cambrian the Baydrag and Lesser Qaratau blocks were parts of larger Mongolian and Kazakh domains [7, 40].

(2) It can be stated with confidence that about 800 Ma ago before the breakdown of Rodinia, the Baydrag and Lesser Qaratau blocks (Mongolian and Kazakh domains) belonged to one of the North Rodinian plates—India, Tarim, or South China.

(3) Lithologic, stratigraphic, and paleontological data allow us to suggest that in the Late Neoproterozoic–Early Cambrian the southern part of the Siberian Platform, Tarim, South China platforms, and most microcontinents in the UMB existed under similar climatic and paleogeographic conditions of warm and shallow-water marine basin.

(4) Widespread carbonate rocks and a single paleomagnetic result [46] show that this hypothetical basin was situated at equatorial latitudes.

(5) According to lithologic and geochemical data [5], the Mongolian and Kazakh domains were sepa-

rated from Siberia and other large cratonic blocks by relatively wide marine basins.

(6) Island arcs were localized at a significant distance from the sialic massifs, and no admixture of tuffaceous material was established in their sedimentary sequences [23].

Summing up the aforesaid, it can be suggested that the scenario of the development of the Ural–Mongolian Belt in the Late Neoproterozoic–Early Cambrian did not include many exotic terranes, which traveled for a great distance crossing wide oceanic basins. At that time, an extensive warm shallow-water basin with an archipelago of continental blocks probably existed to the north of the Siberian Platform (Fig. 8). This system can be compared with the Canadian Arctic Archipelago. The island arcs most likely were located far seaward and conjugated with sialic massifs much later.

ACKNOWLEDGMENTS

We thank our many colleagues from the Institute of Geology and Mineral Resources, Mongolian Academy of Sciences in Ulaanbaatar, in particular Doctor Tomurhuu, for their amicability and hospitality. We are grateful to V.M. Kalugin and other colleagues from the Institute of Geology and Mineralogy, Siberian Branch, Russian Academy of Sciences, for their assistance in organization and conduction of fieldworks and to A.V. Shatsillo and V.E. Pavlova for permission to use their unpublished data. We also thank V.E. Khain (deceased), K.E. Degtyarev, and A.N. Didenko for their constructive criticism. This study was supported by the Russian Foundation for Basic Research (project no. 07-05-00021), the Division of the Earth's Sciences, Russian Academy of Sciences (program no. 10), and the National Science Foundation of the United States (grant EAR05-08597).

REFERENCES

1. S. G. Ankinovich, *Lower Paleozoic of V-Bearing Basin of the North Tien Shan and the Western Margin of Central Kazakhstan* (Acad. Sci. KazSSR, Alma-Ata, 1961), Part 1 [in Russian].
2. V. G. Belichenko, E. F. Letnikova, and N. K. Geletii, "Geochemical Features of Carbonate Deposits in Covers of the Tuva-Mongolia Microcontinent," *Dokl. Akad. Nauk* **364** (1), 80–83 (1999) [*Dokl. Earth Sci.* **364** (1), 1–4 (1999)].
3. V. V. Burashnikov and S. V. Ruzhentsev, "The Sharyngol Upper Riphean–Vendian Rift-Related Complex," *Dokl. Akad. Nauk* **332** (1), 54–57 (1993).
4. V. S. Burtman, "Some Problems Concerning Paleozoic Tectonic Reconstructions in Central Asia," *Geotektonika* **33** (4), 103–112 (1999).
5. S. V. Veshcheva, O. M. Turkina, E. F. Letnikova, and Yu. L. Ronkin, "Geochemical and Sm–Nd Isotopic Characteristics of the Neoproterozoic Terrigenous Rocks of the Tuva-Mongolian Massif," *Dokl. Akad. Nauk* **418** (1), 155–160 (2008) [*Dokl. Earth Sci.* **418** (1), 155–160 (2008)].
6. A. S. Gibsher, E. V. Khain, A. B. Kotov, et al., "The Late Vendian Age of the Hantayshir Ophiolite Complex of Western Mongolia," *Geol. Geofiz.* **42** (8), 1179–1185 (2001).
7. K. E. Degtyarev and A. V. Ryazantsev, "Cambrian Arc-Continent Collision in the Paleozooids of Kazakhstan," *Geotektonika*, **41** (1), 71–96 (2007) [*Geotectonics* **41** (1), 63–86 (2007)].
8. A. N. Didenko, A. A. Mossakovsky, D. M. Pechersky, et al., "Geodynamics of Paleozoic Oceans of Central Asia," *Geol. Geofiz.* **35** (7/8), 59–75 (1994).
9. N. V. Esakova and E. A. Zhegallo, *Biostratigraphy and Fauna of the Lower Cambrian in Mongolia* (Nauka, Moscow, 1996) [in Russian].
10. I. T. Zhuravleva, "Paleobiogeography of the Early Cambrian," in *Paleontology, Paleobiogeography, and Mobilistic Concept* (Knizhn. Izd-vo, Magadan, 1981), pp. 43–51 [in Russian].
11. L. P. Zonenshain, M. I. Kuz'min, and L. M. Natapov, *Tectonics of the Lithospheric Plates of the Territory of the USSR* (Nedra, Moscow, 1990), Vol. 1, [in Russian].
12. E. I. Zubtsov, *Ulutau–Tien Shan Tillite Complex of the Late Precambrian* (Moscow State Univ., Moscow, 1971) [in Russian].
13. A. L. Knipper, *Tectonics of the Baikonur Synclinorium* (Nauka, Moscow, 1963) [in Russian].
14. I. K. Kozakov, E. V. Bibikova, L. A. Neimark, and T. I. Kirnozova, "The Baydrag Block," in *Early Precambrian of the Central Asian Foldbelt* (Dom Nauka, St. Petersburg, 1993), pp. 118–137 [in Russian].
15. V. G. Korolev and R. A. Maksumova, *Precambrian Tillites and Tillitoids of the Tien Shan* (Ilim, Frunze, 1984) [in Russian].
16. A. B. Kotov, I. K. Kozakov, E. V. Bibikova, E. B. Sal'nikova, E. I. Kirnozova, V. P. Kovach, "Duration of Episodes of Regional Metamorphism in Regions of Polycyclic Endogenic Processes: U–Pb Geochronological Study," *Petrologiya* **3** (6), 567–575 (1995).
17. A. B. Kuz'michev, *Tectonic History of the Tuva–Mongolian Massif: Early Baikalian, Late Baikalian, and Early Caledonian Stages* (PROBEL, Moscow, 2004) [in Russian].
18. D. V. Metelkin, I. V. Belonosov, D. P. Gladkochub, et al., "Paleomagnetic Directions in the Intrusions of the Nersa Complex of the Biryusa Sayan Region as a Reflection of Tectonic Events in the Neoproterozoic," *Geol. Geofiz.* **46** (4), 398–413 (2005).
19. A. A. Mossakovsky, S. V. Ruzhentsev, S. G. Samygin, and T. N. Kheraskova, "Central Asian Foldbelt: Geodynamic Evolution and Formation History," *Geotektonika* **27** (6), 3–32 (1993).
20. V. N. Puchkov, *Paleogeodynamics of the Southern and Central Urals* (Dauriya, Ufa, 2000) [in Russian].
21. L. N. Repina, "Paleobiogeography of the Early Cambrian Seas from Trilobites," in *Biostratigraphy and Biogeography of the Paleozoic of Siberia*, Ed. by A.V. Kanygin and N.P. Meshkova (Inst. Geol. Geophys., Novosibirsk, 1985), pp. 5–15 [in Russian].

22. S. V. Ruzhentsev and V. V. Burashnikov, "Tectonics of Salairides of Western Mongolia," *Geotektonika* **29** (5), 25–40 (1995).
23. Yu. K. Sovetov, "Neoproterozoic Rifting and Evolution of Sedimentary Basins in Tarim-Type Microcontinents: The Lesser Karatau, Southern Kazakhstan," in *Types of Sedimentogenesis and Lithogenesis and Their Evolution in the Earth's History* (Inst. Geol. Geophys., Novosibirsk, 2008), Vol. II, pp. 287–289 [in Russian].
24. E. V. Khain, L. A. Neimark, and Yu. V. Amelin, "Caledonian Stage of Remobilization of Precambrian Basement of the Gargan Block, the Eastern Sayan: Isotopic–Geochemical Data," *Dokl. Akad. Nauk* **342** (6), 776–780 (1995).
25. T. N. Kheraskova, S. G. Samygin, S. V. Ruzhentsev, and A. A. Mossakovsky, "Late Riphean Marginal Continental Volcanic Belt of Eastern Gondwana," *Dokl. Akad. Nauk* **342** (5), 661–664 (1995).
26. V. V. Yarmolyuk, V. I. Kovalenko, V. P. Kovach, et al., "Geodynamics of Caledonides in the Central Asian Foldbelt," *Dokl. Akad. Nauk* **389** (3), 1–6 (2003) [*Dokl. Earth Sci.* **389A** (3), 311–316 (2003)].
27. L. D. Ashwal, D. Demaiffe, and T. H. Torsvik, "Petrogenesis of Neoproterozoic Granitoids and Related Rocks from the Seychelles: Evidence for the Case of an Andean-Type Arc Origin," *J. Petrol.* **43**, 45–83 (2002).
28. N. A. Berzin and N. L. Dobretsov, "Geodynamic Evolution of Southern Siberia in Late Precambrian–Early Paleozoic Time," in *Proceedings of the 29th Intern. Geol. Congress on Reconstruction of the Palaeoasian Ocean* (VSP, Utrecht, 1994), pp. 53–70.
29. Y. Chen, B. Xu, S. Zhan, and Y. G. Li, "First Mid-Neoproterozoic Paleomagnetic Results from the Tarim Basin (NW China) and Their Geodynamic Implications," *Precamb. Res.* **133**, 271–281 (2004).
30. J. P. Cogné, "PaleoMac: a Macintosh Application for Treating Paleomagnetic Data and Making Plate Reconstructions," *Geochem. Geophys. Geosyst.* **4** (1), 1007 (2003).
31. D. A. Evans, A. Y. Zhuravlev, C. J. Budney, and J. L. Kirschvink, "Palaeomagnetism of the Bayan Gol Formation, Western Mongolia," *Geol. Mag.* **133**, 487–496 (1996).
32. D. A. D. Evans, Z. X. Li, J. L. Kirschvink, and M. T. D. Wingate, "A High-Quality Mid-Proterozoic Paleomagnetic Pole from South China, with Implications for an Australia–Laurentia Connection at 755 Ma," *Precamb. Res.* **100**, 213–234 (2000).
33. R. A. Fisher, "Dispersion on a Sphere," *Proc. Royal Soc., Ser. A*, **217**, 295–305 (1953).
34. R. B. Hargraves and R. A. Duncan, "Radiometric Age and Paleomagnetic Results from Seychelles Dikes," *Proceedings of the Ocean Drilling Program: Scientific Results* **115**, 119–122 (1990).
35. S. S. Harlan, J. W. Geissman, and L. W. Snee, "Paleomagnetic and $^{40}\text{Ar}/^{39}\text{Ar}$ Geochronologic Data from Late Proterozoic Mafic Dykes and Sills, Montana and Wyoming," USGS Prof. Paper, No. 1580, 1–16 (1997).
36. L. M. Heaman, A. N. Le Cheminant, and R. H. Rainbird, "Nature and Timing of Franklin Igneous Events Canada: Implications for a Late Proterozoic Mantle Plume and the Break-Up of Laurentia," *Earth Planet. Sci. Lett.* **109**, 117–131 (1992).
37. B. C. Huang, B. Xu, C. X. Zhang, et al., "Paleomagnetism of the Baiyisi Volcanic Rocks (Ca. 740 Ma) of Tarim Northwest China: a Continental Fragment of Neoproterozoic Western Australia?," *Precamb. Res.* **142**, 83–92 (2005).
38. M. P. Iglesia-Llanos, J. A. Tait, V. Popov, and A. Ablamasova, "Paleomagnetic Data from Ediacaran (Vendian) Sediments of the Arkhangelsk Region, NW Russia: An Alternative APWP of Baltica for the Late Proterozoic–Early Paleozoic," *Earth Planet. Sci. Lett.* **240**, 732–747 (2005).
39. A. V. Ilyin, "Proterozoic Supercontinent, Its Latest Precambrian Rifting, Break-Up, Dispersal Into Smaller Continents, and Subsidence of Their Margins: Evidence from Asia," *Geology* **18**, 1231–1234 (1990).
40. E. V. Khain, E. V. Bibikova, E. B. Salnikova, et al., "The Palaeo-Asian Ocean in the Neoproterozoic and Early Palaeozoic: New Geochronologic Data and Palaeotectonic Reconstructions," *Precamb. Res.* **122**, 329–358 (2003).
41. T. N. Kheraskova, A. N. Didenko, V. A. Bush, and Yu. A. Volozh, "The Vendian–Early Paleozoic History of the Continental Margin of Eastern Paleogondwana, Palaeoasian Ocean, and Central Asian Foldbelt," *Russ. J. Earth Sci.* **5** (3), 165–184 (2003).
42. V. V. Khomentovsky and A. S. Gibsher, "The Neoproterozoic–Lower Cambrian in Northern Gobi-Altay, Western Mongolia: Regional Setting, Lithostratigraphy, and Biostratigraphy," *Geol. Mag.* **133** (4), 371–390 (1996).
43. J. L. Kirschvink, "The Precambrian Cambrian Boundary Problem: Magnetostratigraphy of the Amadeus Basin, Central Australia," *Geol. Mag.* **115**, 139–150 (1978).
44. J. L. Kirschvink, "The Least-Square Line and Plane and the Analysis of Palaeomagnetic Data," *Geophys. J. Roy. Astron. Soc.* **62**, 699–718 (1980).
45. J. Kosler and P. J. Sylvester, "Present Trends and the Future of Zircon in Geochronology: Laser Ablation ICPMS, Zircon," *Rev. Mineral. Geochem.* **53**, 243–271 (2003).
46. V. A. Kravchinsky, K. M. Konstantinov, and J.-P. Cogne, "Paleomagnetic Study of Vendian and Early Cambrian Rocks of South Siberia and Central Mongolia: Was the Siberian Platform Assembled at this Time?," *Precamb. Res.* **110**, 61–92 (2001).
47. A. Kröner, B. F. Windley, G. Badarh, et al., "Accretionary Growth and Crust Formation in the Central Asian Orogenic Belt and Comparison with the Arabian–Nubian Shield," *Geol. Soc. Amer. Mem.* **200**, 181–209 (2007).
48. N. M. Levashova, J. G. Meert, A. S. Gibsher, and M. L. Bazhenov, "The Origin of the Central Asian Orogenic Belt Microcontinents: Constraints from Paleomagnetism and Geochronology," *Precamb. Res.* 2010 (in press).
49. Z. X. Li, "New Palaeomagnetic Results from the "Cap Dolomite" of the Neoproterozoic Walsh Tillite, Northwestern Australia," *Precamb. Res.* **100**, 359–370 (2000).

50. Z. X. Li, X. H. Li, P. D. Kinny, et al., “Geochronology of Neoproterozoic Syn-Rift Magmatism in the Yangtze Craton South China and Correlations with Other Continents: Evidence for a Mantle Superplume That Broke Up Rodinia,” *Precamb. Res.* **122**, 85–109 (2003).
51. Z. X. Li, D. A. D. Evans, and S. Zhang, “A 90° Spin on Rodinia: Possible Causal Links between the Neoproterozoic Supercontinent, Superplume, True Polar Wander and Low-Latitude Glaciation,” *Earth Planet. Sci. Lett.* **220**, 409–421 (2004).
52. Z. X. Li, S. V. Bogdanova, A. Davidson, et al., “Assembly, Configuration, and Break-Up History of Rodinia: a Synthesis,” *Precamb. Res.* **160**, 179–210 (2008).
53. J. L. Lin, M. D. Fuller, and W. Y. Zhang, “Paleogeography of the North and South China Blocks During the Cambrian,” *J. Geodyn.* **2**, 91–114 (1985).
54. S. Lu, H. Li, C. Zhang, and G. Niu, “Geological and Geochronological Evidence for the Precambrian Evolution of the Tarim Craton and Surrounding Continental Fragments,” *Precamb. Res.* **160**, 94–107 (2008a).
55. S. Lu, G. Zhao, H. Wang, and G. Hao, “Precambrian Basement and Sedimentary Cover of the North China Craton: a Review,” *Precamb. Res.* **160**, 77–93 (2008b).
56. K. R. Ludwig, *User’s Manual for ISOPLOT*, a Geochemical Toolkit for Microsoft Excel Version 3.09.
57. K. V. Mardia, *Statistics of Directional Data* (Academic Press, London, 1972).
58. M. W. McElhinny, “Statistical Significance of the Fold Test in Palaeomagnetism,” *Geoph. J. Roy. Astron. Soc.* **8**, 338–340 (1964).
59. P. L. McFadden and M. W. McElhinny, “The Combined Analysis of Remagnetization Circles and Direct Observations in Palaeomagnetism,” *Earth Planet. Sci. Lett.* **87**, 161–172 (1988).
60. M. O. McWilliams and M. W. McElhinny, “Late Precambrian Palaeomagnetism in Australia: the Adelaide Geosyncline,” *J. Geol.* **88**, 1–26 (1980).
61. J. G. Meert, R. Van der Voo, and T. Payne, “Paleomagnetism of the Catotian Volcanic Province: a New Vendian–Cambrian Apparent Polar Wander Path for North America,” *J. Geophys. Res.* **99** (B3), 4625–4641 (1994).
62. J. G. Meert and T. H. Torsvik, “The Making and Unmaking of a Supercontinent: Rodinia Revisited,” *Tectonophysics* **375**, 261–288 (2003).
63. G. Murthy, C. Gower, M. Tubrett, and R. Patzold, “Paleomagnetism of Eocambrian Long Range Dykes and Double Mer Formation from Labrador, Canada,” *Can. J. Earth Sci.* **29**, 1224–1234 (1992).
64. J. B. Paces and J. D. Miller, Jr., “Precise U–Pb Ages of Duluth Complex and Related Mafic Intrusions, Northeastern Minnesota: Geochronological Insights to Physical, Petrogenetic, Paleomagnetic, and Tectonomagmatic Processes Associated with the 1.1 Ga Midcontinent Rift System,” *J. Geophys. Res.* **98**, 997–14013 (1993).
65. H. C. Palmer, W. R. A. Baragar, M. Fortier, and J. H. Foster, “Paleomagnetism of Late Proterozoic Rocks, Victoria Island, Northwest Territories, Canada,” *Can. J. Earth Sci.* **20**, 1456–1469 (1983).
66. J. K. Park, D. K. Norris, and A. Larochelle, “Paleomagnetism and the Origin of the Mackenzie Arc of Northwestern Canada,” *Can. J. Earth Sci.* **26**, 2194–2203 (1989).
67. J. K. Park, “Palaeomagnetic Constraints on the Position of Laurentia from Middle Neoproterozoic to Early Cambrian Times,” *Precamb. Res.* **69**, 95–112 (1994).
68. V. E. Pavlov, V. A. Kravchinsky, A. V. Shatsillo, and R. Yu. Petrov, Paleomagnetism of the Upper Riphean Rocks of Turukhansk, Olenek and Uda Sis-Sayan Regions: implications to Neoproterozoic drift of the Siberian platform (in preparation).
69. S. A. Pisarevsky, Z. X. Li, K. Grey, and M. K. Stevens, “A Palaeomagnetic Study of Empress 1A, a Stratigraphic Drillhole in the Officer Basin: Evidence for a Low-Latitude Position of Australia in Neoproterozoic,” *Precamb. Res.* **110**, 93–108 (2001).
70. S. A. Pisarevsky, M. T. D. Wingate, M. K. Stevens, and P. W. Haines, “Paleomagnetic Results from the Lancer-1 Stratigraphic Drill Hole, Officer Basin, Western Australia, and Implications for Rodinia Reconstructions,” *Austr. J. Earth Sci.* **54**, 561–572 (2007).
71. V. Popov, A. Iosifidi, A. Khramov, et al., “Paleomagnetism of Upper Vendian Sediments from the Winter Coast, White Sea Region, Russia: Implications for the Paleogeography of Baltica During Neoproterozoic Times,” *J. Geophys. Res.* **107**, 2315 (2002).
72. V. Popov, A. Khramov, and V. Bachtadze, “Paleomagnetism, Magnetic Stratigraphy and Petromagnetism of the Upper Vendian Sedimentary Rocks in the Sections of the Zolotitsa River and in the Verkhotina Hole, Winter Coast of the White Sea, Russia,” *Russian J. Earth Sci.* **7**, 1–29 (2005).
73. T. Radhakrishna and M. Joseph, “Late Precambrian (850–800 Ma) Paleomagnetic Pole for the South Indian Shield from the Harohalli Alkaline Dykes; Geotectonic Implications for Gondwana Reconstructions,” *Precamb. Res.* **80**, 77–87 (1996).
74. Z. Q. Rui and J. D. A. Piper, “Paleomagnetic Study of Neoproterozoic Glacial Rocks of the Yangzi Block; Paleolatitudes and Configuration of South China in the Late Proterozoic Supercontinent,” *Precamb. Res.* **85**, 173–199 (1997).
75. A. M. C. Şengör, B. A. Natal’in, “Paleotectonics of Asia: Fragments of a Synthesis,” in *The Tectonic Evolution of Asia* (Cambridge Univ. Press, Cambridge, 1996), pp. 486–640.
76. A. V. Shatsillo, A. N. Didenko, and V. E. Pavlov, “Paleomagnetism of Vendian Deposits of the Southwestern Siberian Platform,” *Russian J. Earth Sci.* **8**, ES2003 (2006).
77. A. Simonetti, L. M. Heaman, R. P. Hartlaub, R. A. Creaser, T. G. MacHattie, and C. Bohm, “U–Pb Zircon Dating by Laser Ablation-MC-ICP-MS Using a New Multiple Ion Counting Faraday Collector Array,” *J. Analyt. Atom. Spectr.* **20**, 677–686 (2005).
78. L. E. Sohl, N. Christie-Blick, and D. V. Kent, “Paleomagnetic Polarity Reversals in Marinoan (Ca 600 Ma) Glacial Deposits of Australia: Implications for the Duration of Low-Latitude Glaciation in Neoproterozoic Time,” *Geology* **111**, 1120–1139 (1999).

79. G. M. Stampfli and G. D. Borel, "A Plate Tectonic Model for the Paleozoic and Mesozoic Constrained by Dynamic Plate Boundaries and Restored Synthetic Oceanic Isochrones," *Earth Planet. Sci. Lett.* **196**, 17–33 (2002).
80. D. T. A. Symons and A. D. Chiasson, "Paleomagnetism of the Callander Complex and the Cambrian Apparent Polar Wander Path for North America," *Can. J. Earth Sci.* **28**, 355–363 (1991).
81. E. I. Tanczyk, P. Lapointe, W. A. Morris, and P. W. Schmidt, "A Paleomagnetic Study of the Layered Mafic Intrusions at Sept-Iles, Quebec," *Can. J. Earth Sci.* **24**, 1431–1438 (1987).
82. T. H. Torsvik, L. M. Carter, L. D. Ashwal, et al., "Rodinia Refined or Obscured: Palaeomagnetism of the Malani Igneous Suite (NW India)," *Precamb. Res.* **108**, 319–333 (2001a).
83. T. H. Torsvik, L. D. Ashwal, R. D. Tucker, and E. A. Eide, "Neoproterozoic Geochronology and Palaeogeography of the Seychelles Microcontinent: the India Link," *Precamb. Res.* **110**, 47–59 (2001b).
84. J. J. Veevers, "Gondwanaland from 650–500 Ma Assembly Through 320 Ma Merger in Pangea to 185–100 Ma Breakup: Supercontinental Tectonics via Stratigraphy and Radiometric Dating," *Earth-Sci. Rev.* **68**, 1–132 (2004).
85. H. J. Walderhaug, T. H. Torsvik, E. A. Eide, et al., "Geochronology and Paleomagnetism of the Hunnedalen Dykes, SW Norway: Implications for the Sveconorwegian Apparent Polar Wander Loop," *Earth Planet. Sci. Lett.* **169**, 71–83 (1999).
86. H. J. Walderhaug, T. H. Torsvik, and E. Halvorsen, "Geomagnetism, Rock Magnetism and Palaeomagnetism. The Egersund Dykes (SW Norway): a Robust Early Ediacaran (Vendian) Palaeomagnetic Pole from Baltica," *Geophys. J. Int.* **168**, 935–948 (2007).
87. M. R. Walter, J. J. Veevers, C. R. Calver, et al., "Dating the 840–544 Ma Neoproterozoic Interval by Isotopes of Strontium, Carbon and Sulfur in Seawater, and Some Interpretative Models," *Precamb. Res.* **100**, 371–432 (2000).
88. A. B. Weil, J. W. Geissman, and R. Van der Voo, "Paleomagnetism of the Neoproterozoic Chuar Group, Grand Canyon Supergroup, Arizona: Implications for Laurentia's Neoproterozoic APWP and Rodinia Break-Up," *Precamb. Res.* **129**, 71–92 (2004).
89. I. S. Williams, "U–Th–Pb Geochronology by Ion Microprobe," *Rev. Econ. Geol.* **7**, 1–35 (1998).
90. M. T. D. Wingate and J. W. Giddings, "Age and Paleomagnetism of the Mundine Well Dyke Swarm, Western Australia: Implications for an Australia–Laurentia Connection at 750 Ma," *Precamb. Res.* **100**, 335–357 (2000).
91. A. Yakubchuk, A. Cole, R. Seltmann, and V. V. Shatov, "Tectonic Setting, Characteristics, and Regional Exploration Criteria for Gold Mineralization in the Altaid Tectonic Collage: the Tien Shan Province as a Key Example," *Soc. Econ. Geol. Spec. Publ.* **9**, 177–201 (2002).
92. A. Yakubchuk, "Re-Deciphering the Tectonic Jigsaw Puzzle of Northern Eurasia," *J. Asian Earth Sci.* **32**, 82–101 (2008).
93. S. Zhang, Z. X. Li, and H. Wu, "New Precambrian Palaeomagnetic Constraints on the Position of the North China Block in Rodinia," *Precamb. Res.* **144**, 213–238 (2006).
94. J. D. A. Zijderveld, "AC Demagnetization of Rocks: Analysis of Results," in *Methods in Paleomagnetism* (Elsevier, Amsterdam, 1967), pp. 254–286.

Reviewers: V.E. Khain[†] and K.E. Degtyarev